Available online at www.sciencedirect.com
SCIENCE DIRECT®
Journal of Nuclear Materials 345 (2005) 31–40
journal of nuclear materials
www.elsevier.com/locate/jnucmat

Vitrification and testing of a Hanford high-level waste sample. Part 2: Phase identification and waste form leachability

P. Hrma *, J.V. Crum, P.R. Bredt, L.R. Greenwood, B.W. Arey, H.D. Smith

Pacific Northwest National Laboratory, Richland, WA 99354, USA

Received 25 October 2004; accepted 18 March 2005

Abstract

A sample of Hanford high-level radioactive waste from Tank AZ-101 was vitrified into borosilicate glass and tested to demonstrate its compliance with regulatory requirements. Compositional aspects of this study were reported in Part 1 of this paper. This second and last part presents results of crystallinity and leachability testing. Crystallinity was quantified in a glass sample heat treated according to the calculated cooling curve of glass at the centerline of a Hanford Waste Treatment Plant canister. By quantitative X-ray diffraction analysis and image analysis applied to scanning electron microscopy micrographs, the sample contained 7 mass% of spinel, a solid solution of franklinite, trevorite, and other minor spinels. Glass leachability was measured with the product consistency test and the toxicity characteristic leaching procedure. Measured data and model estimates were in reasonable agreement. Leachability results were close to those obtained for the non-radioactive simulant. Models were used to elucidate the effects of glass composition of spinel formation and to estimate effects of spinel formation on glass leachability.

PACS: 61.43.Fs; 81.05.Kf; 82.80.−d

1. Introduction

Radioactive waste currently stored in underground tanks at Hanford will be separated into high-level and low-activity portions, and both wastes will be vitrified for permanent disposal. The high-level waste (HLW) glass will be poured into canisters and shipped to the repository. To demonstrate that the glass produced by vitrifying HLW currently stored in Tank AZ-101 will be processable in electric melters and meet regulatory specifications, a pre-processed sample of this waste was blended with Cs and Tc secondary wastes, mixed with mineral additives, and vitrified, obtaining 163 g of AZ-101 HLW glass. The outcome of the chemical and radiochemical analyses of this glass was reported in Part 1 of this paper [1]. Briefly, the waste-loading fraction in the glass was 33.2 mass%; its targeted and analyzed chemical compositions are given in Table 1. This second and last part reports the outcome of testing the glass sample for crystallinity and leachability. As seen in Table 1, the presence of spinel-forming components, Fe_2O_3, ZnO, NiO, MnO, and Cr_2O_3, in the glass indicates that spinel may precipitate during processing and is likely to be

* Corresponding author. Tel.: +1 509 376 5092; fax: +1 509 376 3108.
E-mail address: pavel.hrma@pnl.gov (P. Hrma).

0022-3115/$ - see front matter © 2005 Elsevier B.V. All rights reserved.
doi:10.1016/j.jnucmat.2005.03.025

Table 1
Averaged best analytical estimates and target compositions for the AZ-101 HLW glass composition in mass fractions of oxides and halides [1]

	Analysis	Target		Analysis	Target		Analysis	Target
SiO_2	0.4430	0.4469	P_2O_5	0.0045	0.0040	RuO_2	0.0008	0.0007
Na_2O	0.1058	0.1187	MnO	0.0030	0.0027	BaO	0.0006	0.0007
Fe_2O_3	0.1200	0.1116	La_2O_3	0.0047	0.0026	PbO	0.0004	0.0004
B_2O_3	0.1008	0.1063	Ce_2O_3	0.0006	0.0024	Ag_2O	0.0001	0.0004
Al_2O_3	0.0823	0.0733	Nd_2O_3	0.0017	0.0020	Cl	0.0003	0.0003
Li_2O	0.0373	0.0376	SnO_2	0.0023	0.0019	CuO	0.0002	0.0003
ZrO_2	0.0374	0.0338	SrO	0.0020	0.0016	F	0.0002	0.0002
ZnO	0.0199	0.0201	Cr_2O_3	0.0013	0.0014	Rh_2O_3	0.0008	0.0002
UO_3	0.0090	0.0092	K_2O	0.0002	0.0013	TiO_2	0.0002	0.0002
CdO	0.0068	0.0064	MgO	0.0011	0.0011	Y_2O_3	0.0002	0.0002
NiO	0.0054	0.0049	SO_3	0.0011	0.0011	Bi_2O_3	0.0002	0.0001
CaO	0.0047	0.0042	PdO	0.0010	0.0010	CoO	0.0001	0.0001

present in the final glass. To identify and quantify crystalline phases expected in a canister filled with AZ-101 HLW glass, the glass was slowly cooled, following the canister centerline cooling history (determined by model calculation), and then analyzed with quantitative X-ray diffraction (XRD), scanning electron microscopy (SEM), energy dispersive spectroscopy (EDS), and image analysis. The product consistency test (PCT) [2] and the toxicity characteristic leaching procedure (TCLP) [3] were performed (PCT on canister centerline cooled glass and TCLP on quenched glass) to demonstrate that the glass met acceptability conditions associated with its chemical durability [4]. No other tests were performed so far, but the remaining glass sample was stored for future testing if needed.

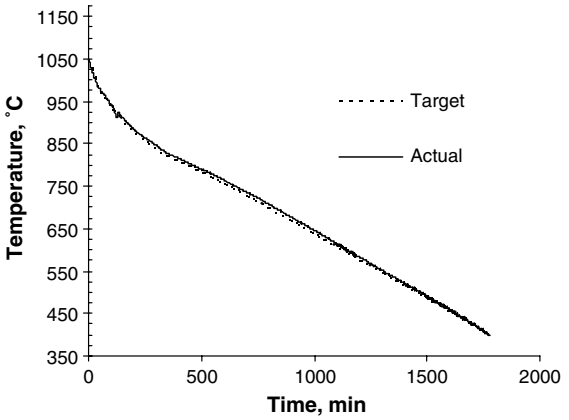

Fig. 1. Hanford canister centerline glass cooling curve (target) and actual heat-treatment curve of AZ-101 glass sample.

2. Experimental

A 20-g AZ-101 HLW glass monolithic sample was heat treated in a $25 \times 25 \times 25$-mm Pt10%Rh box following the canister centerline cooling curve approximated by a series of linear time–temperature segments (Table 2).

Table 2
Segmented approximate centerline cooling curve for a canister of HLW glass at Hanford[a]

Segment number	Segment end time, min	Segment start temperature, °C	Cooling rate, °C/min
1	45	1050	−1.556
2	107	980	−0.806
3	200	930	−0.591
4	329	875	−0.388
5	527	825	−0.253
6	707	775	−0.278
7	1776	725	−0.304

[a] Data in this table are due to courtesy of L. Petkus.

Fig. 1 compares the targeted cooling curve with the thermocouple reading. After the heat treatment, a 2-g triangular prism was cut from the monolith with a low-speed diamond wafering saw. From the prism, samples were taken for SEM (VG Elemental Shielded PQ2 with EDS) and for XRD (Scintag X-ray diffractometer, Model PAD V, employing Cu Kα radiation). For SEM, an $\sim 1 \times 3$-mm sliver of glass was chipped, potted in epoxy, and polished; 20 keV was used for EDS analysis and 10 keV for image processing. For XRD, ~20 mg of glass was crushed, mixed with 3 mg of powdered corundum as an internal standard, blended with a mortar and pestle, and mixed into a collodion solution. The samples were made small deliberately to reduce radiation levels. The 2θ XRD scan ranged from 10° to 70°, proceeding in 0.04° steps with a 5-s dwell at each step. For comparison, XRD was also performed on a quenched glass sample (with 0.02° steps and a 20-s dwell). Crystal fraction was determined by Rietveld cell refinement using Riqas software.

The 7-day 90 °C PCT was performed following the American Society for Testing and Materials (ASTM) procedure [2] on AZ-101 HLW slowly cooled glass, the environmental assessment (EA) standard reference glass [5], and blanks. All measurements were done in triplicate. The glass was ground in an automated alumina grinding chamber and sieved through −100 to +200 mesh stainless steel sieves to obtain the grain-size fraction of 75–150 μm that was subsequently ultrasonically cleaned with deionized water followed with ethanol, and dried in an oven at 90 °C. A 1.5 g portion of the cleaned glass particles was placed into a 22-mL container of desensitized (by precipitating chromium carbide in the grain boundaries) Type 304L stainless steel (Fig. 2), filled with 15 mL of deionized water, sealed, and kept for 7 days at 90 °C. The initial and final solution pH was taken with an Orion Research Ion Analyzer, Model 720, calibrated with Fisher buffer solutions of pH = 4.00, and 7.00 before use and Oakton buffer solutions 7.00 and 10.00 after use. Aliquots of the solution were filtered through a 0.45-μm filter, acidified with 1 vol.% of HNO_3, and submitted for analysis with inductively coupled argon plasma atomic emission spectrometer (ICP-AES) (Thermo Jarrell-Ash, Model 61).

For the TCLP test, a 10-g sample of AZ-101 HLW quenched glass was crushed to pass through a 9.5-mm (USA $^3/_8$ in. Mesh) sieve and placed into an extractor vessel with 200 mL of extraction fluid #1 (5.7 mL of glacial acetic acid and 64.3 mL of 1 N sodium hydroxide diluted to 1 L; pH = 4.93 ± 0.05 [3]). From the extract, preserved with concentrated HNO_3, 45-mL aliquots were taken for two acid digestions, one with HNO_3 and HCl and the other with HNO_3 alone, and ~1.5 mL aliquots were taken for Hg analysis. Extracts were analyzed with ICP-AES except for Tl that was analyzed with ICP mass spectroscopy and for Hg that was analyzed with cold vapor atomic absorption spectroscopy. Preparative quality control samples included blanks, duplicates, blank spikes, matrix spikes, and laboratory control standards.

Fig. 2. Stainless steel container for PCT: vessel, lid, Teflon gasket, nickel-plated brass, nut, and screw.

3. Results

3.1. Crystalline phases

As seen in Fig. 3, the XRD pattern of the slowly cooled glass shows a broad amorphous hump with a number of peaks identified as corundum (an internal standard) and various spinels. Two unidentified peaks were matched with a cadmium silicate structure, but no evidence of cadmium silicate was found with SEM. However, cadmium silicate is unlikely to precipitate from the HLW glass and was never observed even in HLW glasses of extreme compositions. Quantitative XRD analysis detected only 7.1 mass% of spinel, predominantly trevorite, in slowly cooled AZ-101 HLW glass; the quenched glass had a barely detectable trace of the spinel.

As SEM micrographs (Fig. 4) show, most of the spinel crystals were 0.5–3 μm in size. Table 3 shows the estimate of spinel composition based on the EDS spectrum of a typical crystal (Fig. 5); sample radiation somewhat shifted the peaks. Trevorite ($NiFe_2O_4$) appears to be the dominant simple spinel. Table 3 estimate corresponds to the chemical formula

$$Ni(II)_{0.48}Zn(II)_{0.32}Fe(II)_{0.57}Fe(III)_{1.50}Cr(III)_{0.20}Mn(III)_{0.06}O_4$$

Provided that spinel is the only crystalline phase in the glass, the mass-balance equation for each component can be written in the form

$$c_i c_S + m_i(1 - c_S) = g_i \quad (i = 1, 2, \ldots, N), \tag{1}$$

where c_i is the ith component mass fraction in spinel, c_S is the spinel mass fraction in glass, m_i is the ith amorphous matrix component mass fraction, and g_i is the ith component mass fraction in the crystal-free glass. The c_i values listed for Cr_2O_3 and NiO in Tables 1 and 3 with $c_S = 0.071$, do not satisfy Eq. (1) because $c_i c_S > g_i$ for these elements, i.e., the amount of these elements in spinel appears larger than their content in the original glass. This implies that either the average composition of spinel is different from that obtained from the EDS for a single crystal or the spinel fraction is lower than the value obtained from XRD data.

To check the value of the spinel content in the glass sample, we applied image analysis to SEM micrographs. Crystal fraction was determined on 12 randomly selected frames (6 images of 86 × 71 μm and 6 images of 43 × 35 μm) to be 3.55 ± 0.50 vol.%, see Table 4 (the area fraction and volume fraction are identical for the isotropic crystals of spinel). The mass fraction, is related to the volume fraction, v_S, by the formula

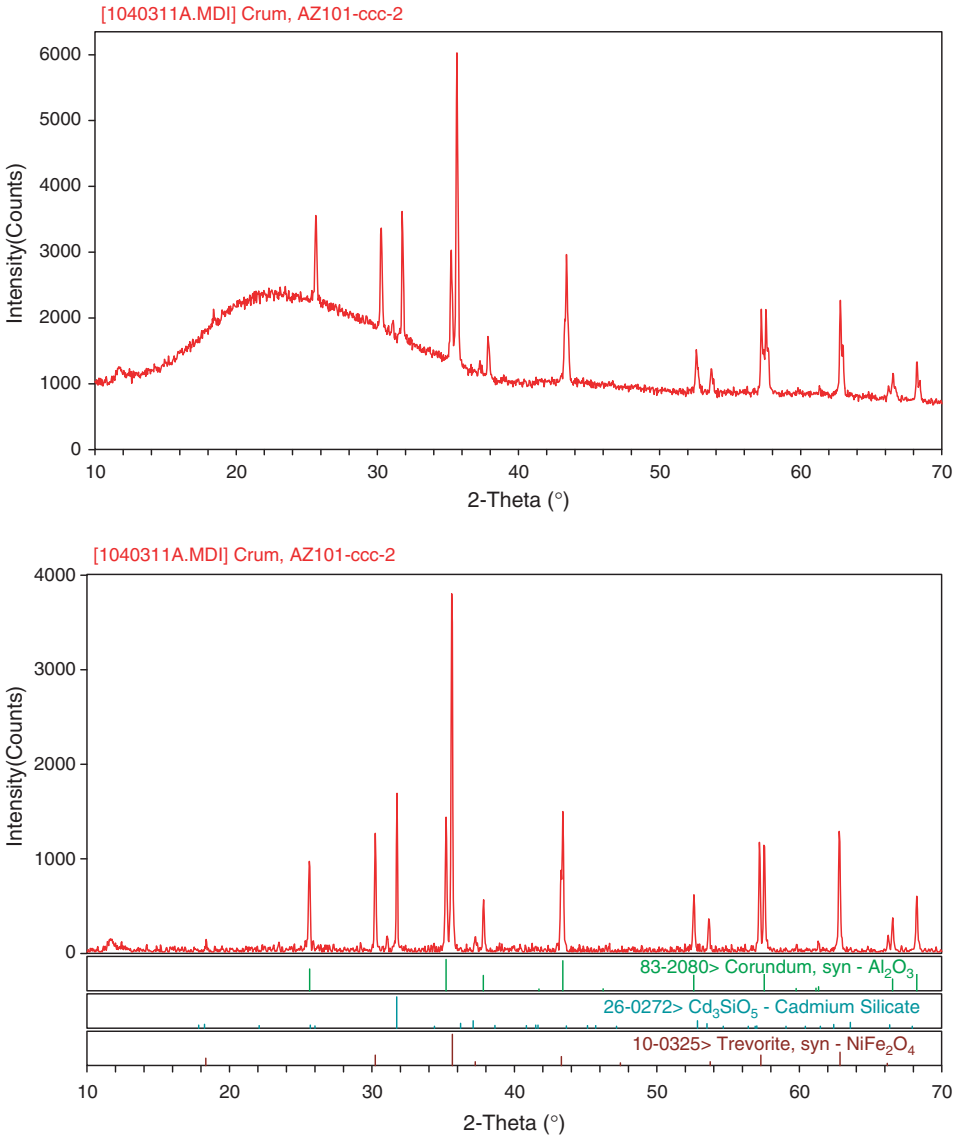

Fig. 3. XRD pattern of AZ-101 HLW slowly cooled glass showing amorphous hump (top) and crystalline phases (bottom – amorphous hump subtracted); corundum was an internal standard.

$$c_S = \left[1 + \frac{\rho_M}{\rho_S}\left(\frac{1}{v_S} - 1\right)\right]^{-1}, \tag{2}$$

where ρ_M and ρ_S are the amorphous matrix and spinel density, respectively. The amorphous matrix density was estimated from composition from the formula

$$\rho_M = \frac{1}{\sum_{i=1}^{N} \frac{v_i m_i}{M_i}}, \tag{3}$$

where v_i is the ith glass component partial molar volume (Table 5), M_i is the ith component molecular mass, and N is the number of components. Because m_i values must be positive for each spinel component, the composition of spinel was modified as follows. Mass fractions of Cr_2O_3 and NiO is spinel were decreased to a value that leaves 2% of total Cr_2O_3 and NiO from the original glass in the glass matrix. Mass fractions of Fe_2O_3, Mn_2O_3, and ZnO were increased to compensate for the decrease in Cr_2O_3 and NiO, but were left in unchanged proportion. The modified composition is shown in Table 3. Using trevorite density, 5165 kg/m^3 [6], for spinel and connecting Eqs. (1)–(3), we finally obtained for the spinel mass fraction in glass the value $c_S = 0.0672 \pm 0.0094$. This value is in good agreement with $c_S = 0.071$ from quantitative XRD analysis.

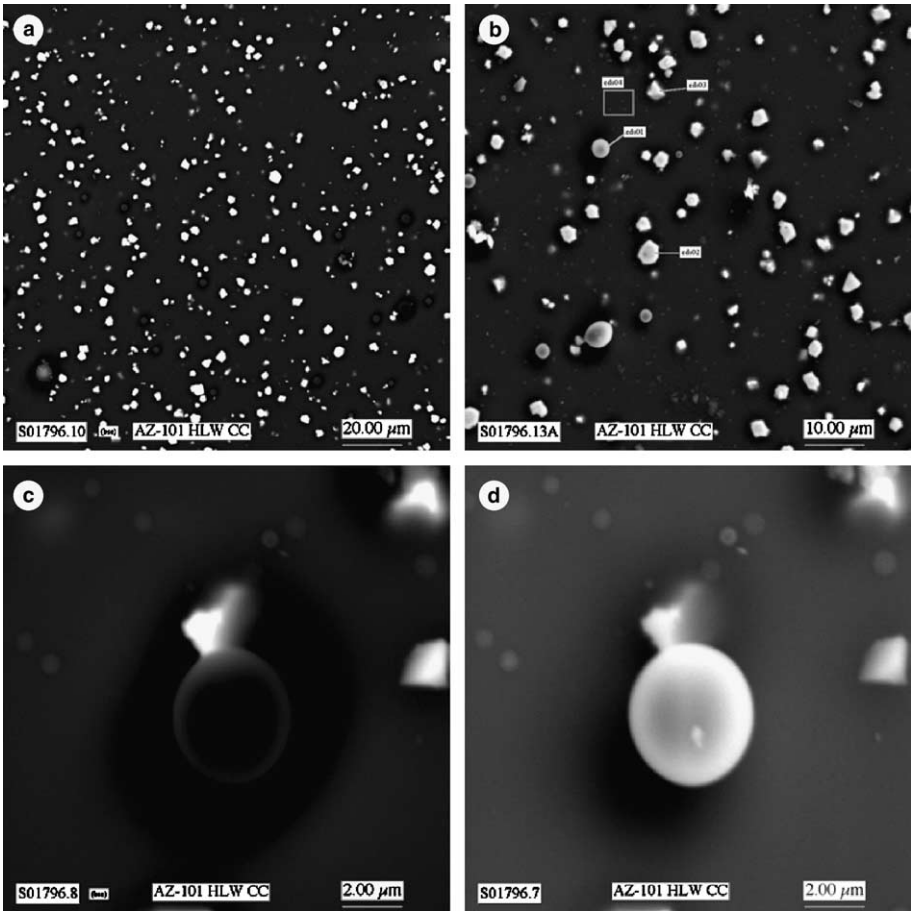

Fig. 4. AZ-101 HLW glass SEM image: (a) and (b) spinel crystals and gas bubbles; (c) and (d) a backscattered and a secondary electron image of a bubble.

Table 3
Estimated spinel composition

	Mass fraction	
	Measured[a]	Modified[b]
Cr_2O_3	0.062	0.020
FeO	0.168	0.637
Fe_2O_3	0.496	0.131
Mn_2O_3	0.018	0.021
NiO	0.149	0.069
ZnO	0.108	0.123

[a] Estimated from EDS.
[b] Modified to meet mass balance constraint.

For the modified composition, the spinel formula is

$$Ni(II)_{0.22}Zn(II)_{0.36}Fe(II)_{0.43}Fe(III)_{1.88}Cr(III)_{0.06}Mn(III)_{0.06}O_4$$

The dominant simple spinel in this solid solution is franklinite ($ZnFe_2O_4$) rather than trevorite.

Somewhat intriguing are the smooth spherical or elliptical objects seen in Fig. 4(a) and (b) and shown in a higher magnification in Fig. 4(c) (a backscattered image) and 4(d) (a secondary electron image). These objects are most likely gas bubbles: their composition

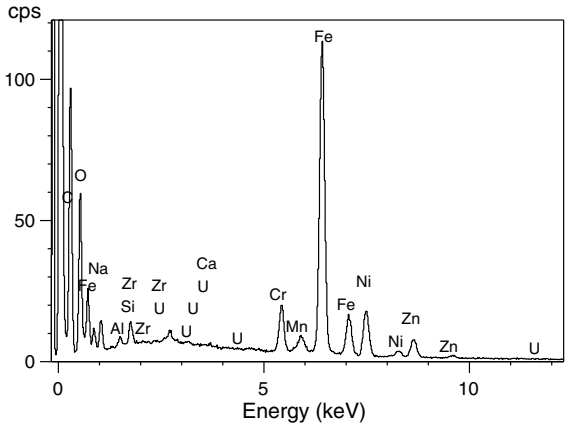

Fig. 5. EDS spectrum of spinel crystal in AZ-101 HLW glass.

Table 4
Evaluation of spinel fraction in AZ-101 HLW glass from image analysis of SEM micrographs

Spinel area fraction	
Average	0.0355
Minimum	0.0296
Maximum	0.0470
Standard deviation	0.0050
Relative error	0.14
Number of frames	12
Quenched glass density, kg/m^3	2712
Spinel density, kg/m^3	5165
Spinel mass fraction	0.0673
Standard deviation	0.0094

Table 5
Partial molar volumes (v_i) of glass components [8]

	v_i, m/kmol		v_i, m/kmol
Al_2O_3	46.15	MnO	13.18
B_2O_3	30.05	Na_2O	19.83
BaO	18.87	NiO	12.67
CaO	15.21	SiO_2	25.32
F	7.53	SrO	17.61
Fe_2O_3	39.16	TiO_2	17.96
K_2O	37.74	ZnO	15.07
Li_2O	9.94	ZrO_2	27.08
MgO	13.03	Others[a]	42.81

[a] Others are all remaining components.

is indistinguishable from that of the glass matrix (Fig. 6). Dark areas around crystals (Fig. 4(b)) can be associated with concentration layers depleted of Fe, Ni, and other spinel-forming components. Dark areas around bubbles (Fig. 4(c)) are most likely artifacts associated with sample preparation (polishing, coating) or localized charging caused by insufficient conductive coating of bubble surfaces.

Only 1.8 vol.% spinel, corresponding to 3.4 mass%, was detected in the non-radioactive simulant glass HLW98-95 [7] subjected to the cooling schedule defined in Table 2. Model calculations [8] resulted in a higher liquidus temperature for AZ-101 HLW glass (1129 °C) than for the simulant (1054 °C). According to the model coefficients listed in Table 6, this 74 °C difference was caused by the cumulative effect of relatively minor composition differences in several spinel-promoting components: Al_2O_3 accounts for 32 °C, Fe_2O_3 for 23 °C, ZrO_2 for 6 °C, and Ni for 5 °C. Another significant difference between AZ-101 HLW and HLW98-95 glasses is that the former contained four times as much $RuO_2 + Rh_2O_3$, which are sparsely soluble components that nucleate spinel [9]. Hence, spinel formation was favored both thermodynamically and kinetically in the radioactive glass.

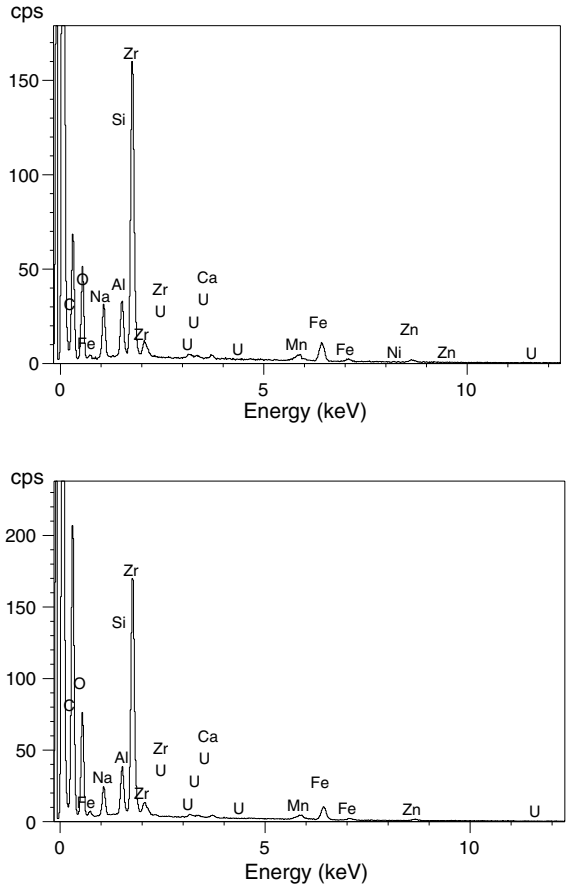

Fig. 6. EDS spectra of AZ-101 HLW glass (top) and glass bubble (bottom).

Table 6
Liquidus temperature coefficients[a] [8]

Element	T_i, °C	Element	T_i, °C	Element	T_i, °C
Ag	5576	La	4885	S	−5493
Al	3210	Li	275	Sb	2662
As	778	Mg	2699	Se	−1100
B	42	Mn	1316	Si	1041
Ba	616	Mo	1931	Sm	4809
Bi	4757	Na	−222	Sr	909
Ca	1226	Nd	4838	Te	3540
Cd	5122	Ni	13675	Th	4188
Ce	4059	P	−2021	Ti	2469
Co	4650	Pb	5340	U	2592
Cr	33271	Pd	5039	V	2364
Cs	−881	Pr	4854	W	1987
Cu	4890	Rb	−802	Y	4745
Fe	3659	Rh	4176	Zn	4688
K	−733	Ru	3408	Zr	3714

[a] A liquidus temperature is given by the formula $T_L = \sum_{i=1}^{P} T_i x_i$, where x_i is the electropositive element mole fraction, such that $1 = \sum_{i=1}^{P} x_i$, and P is the number of electropositive elements in the glass.

3.2. PCT

Tables 7 and 8 summarize the 7-day 90 °C PCT results for AZ-101 HLW glass and for EA glass. More details, including quality control data, are in Ref. [10]. The normalized releases were calculated using the equation

$$r_i = \frac{c_i - c_{Bi}}{g_i \sigma}, \tag{4}$$

where r_i is the ith element normalized release, c_i is the ith element concentration in PCT solution, c_{Bi} is the ith element concentration in the blank, g_i is the ith element mass fraction in glass, and σ is the glass surface-to-solution volume ratio ($\sigma = 2000\ m^{-1}$). The normalized releases of B, Li, and Na from AZ-101 HLW glass, 0.26–0.33 g/m^2, are very low, 5–11% of the corresponding releases of the EA standard reference glass. Somewhat higher releases from EA glass obtained by Jantzen et al. [5] are attributable to the non-radioactive environment [11].

The ith element normalized release is equivalent to the mass of glass per unit glass-solution interface area that contained that element before it was released. The corresponding thickness layer of glass, or the thickness lost provided dissolution was congruent, is $d_i = r_i/\rho_G$ where ρ_G is the glass density. The density of AZ-101 HLW glass was not measured; its value, estimated by applying Eq. (3) to the analyzed glass composition listed in Table 1, is 2712 kg/m^3 (this value is virtually identical to that measured for the non-radioactive simulant [12], 2713 kg/m^3). With this density, the thickness of AZ-101 HLW glass dissolved during the 7-day PCT is ~0.1 μm. Note that 7-day PCT data do not allow any conclusions about the rate of dissolution or extrapolation to longer time periods because glass corrosion proceeds through various stages, and the process is non-linear and initially incongruent [13,14].

Table 9 lists PCT data for HLW98-95 non-radioactive simulant [12], showing that PCT releases from the slowly cooled simulant are nearly identical to those from quenched glass, thus indicating the negligible impact of spinel formation during slow cooling. Releases from slowly cooled HLW98-95 simulant are marginally higher than those from AZ-101 HLW glass, by 0.04 g/m^2 for alkalis and by 0.09 g/m^2 for B, even though the PCT solution pH was higher (11.0) for the simulant.

PCT model calculations can be used for estimating effects that have not been directly measured, such as the impact of spinel precipitation or composition variations. According to a recently updated model [15,16]

$$r_j = \exp\left(\frac{\sum_{i=1}^{N} b_{ij} g_i}{\sum_{i=1}^{N} g_i}\right), \tag{5}$$

where j stands for B, Li, and Na, b_{ij} is the ith component coefficient for jth element release, g_i is the ith component mass fraction in glass, and N is the number of components in glass for which the model was fit. The b_{ij} values are listed in Table 10. Because spinel has a high chemical durability, the PCT releases from the glass with spinel are determined by the composition of the amorphous

Table 7
PCT results for AZ-101 HLW glass

	g_i, fraction	c_i, g/m^3	r_i, g/m^2	σ_i, g/m^2
B	0.0313	16.3	0.260	0.010
Li	0.0173	11.6	0.333	0.016
Na	0.0785	40.6	0.256	0.033
Si	0.2070	64.0	0.154	0.004
pH		9.41		

Table 8
PCT results for EA glass

	g_i, fraction	c_i, g/m^3	r_i, g/m^2	σ_i, g/m^2	r_i,[a] g/m^2	σ_i,[a] g/m^2
B	0.0351	398	5.67	1.51	8.36	0.61
Li	0.0198	123	3.11	0.46	4.8	0.37
Na	0.1246	1009	4.05	0.66	6.67	0.45
Si	0.2278	719	1.58	0.21	1.96	0.19
pH			11.6		11.85	

[a] Reported in [5].

Table 9
Calculated and measured normalized release (r_j) in g/m^2 from AZ-101 HLW and HLW98-95 quenched and slowly cooled glass [12]

	Quenched				Heat treated		
	AZ-101 HLW[a]	HLW98-95[a]	HLW98-95[b]	Target[c]	AZ-101 HLW[d]	AZ-101 HLW[b]	HLW98-95[b]
B	0.428	0.706	0.277	0.599	0.451	0.260	0.166
Li	0.286	0.465	0.293	0.445	0.399	0.333	0.290
Na	0.377	0.637	0.230	0.549	0.410	0.256	0.217

[a] Based on Eq. (5) with the g_i values from chemical analysis.
[b] Measured values.
[c] Based on Eq. (5) with targeted g_i values.
[d] Based on Eqs. (1) and (5) with g_i values from chemical analysis.

Table 10
PCT component coefficients to obtain r_j ($j \equiv$ B, Li, Na) in g/m^2 from Eq. (5) [8]

	$b_{i\mathrm{B}}$	$b_{i\mathrm{Li}}$	$b_{i\mathrm{Na}}$
Al_2O_3	−10.19	−7.76	−9.86
B_2O_3	5.58	3.27	2.47
BaO		16.48	
CaO	−12.4	−17.26	−6.85
Fe_2O_3	−1.9	−4.69	−2.67
K_2O		120.43	
Li_2O	10.97	11.55	11.71
MgO		−25.16	
Na_2O	13	10.78	16.88
SiO_2	−4.47	−3.06	−4.88
SrO		−3.4	−11.17
ThO_2	−124.03		−115.93
TiO_2		−44.4	
UO_2		4.12	
ZnO		−10.46	
ZrO_2		−7.76	

matrix that can be obtained from Eq. (1). Applying Eq. (5) to m_i instead of g_i results in estimates summarized in Table 9. One can observe that (1) calculated PCT releases from the target glass are 40–56% higher than those from the actually made glass, (2) calculated PCT releases from the slowly cooled glass are 5–40% higher than those from the quenched glass (assuming quenched glass is crystal-free), (3) the model overpredicts measured values by 20–70% (based on calculated releases from the amorphous matrix), and (4) releases predicted by the model for quenched simulant are 2–3 times higher than the corresponding measured values.

Table 1 shows that AZ-101 HLW glass made had a higher content of Al_2O_3 and Fe_2O_3 and a lower content of B_2O_3 and Na_2O than the target; by Table 3, spinel removes Fe_2O_3 and ZnO from the glass. These compositional shifts are responsible for differences in the calculated PCT releases: according to Table 10, Al_2O_3 and Fe_2O_3 decrease PCT releases while B_2O_3 and Na_2O increase them; furthermore, ZnO strongly decreases Li release without having a significant effect on B and Na release. These effects can explain most, but not all, differences in PCT responses. As discussed in Ref. [17], several additional factors, such as concentration gradients, internal stresses, and whether fracture surfaces pass through the crystals or avoid them, affect PCT releases from glasses with crystals.

3.3. TCLP

TCLP data are summarized in Table 11 together with the Universal Treatment Standard (UTS) limits and US Environmental Protection Agency (EPA) delisting limits for the elements that exist in HLW glasses. The UTS limits are applicable only for Be, Ni, Sb, and Tl; all other

Table 11
Summary of TCLP results

	Average concentration,[a] g/m^3		EPA delisting limits, g/m^3	UTS limit,[b] g/m^3
Ag		U	3.07	0.14
As		U	3.08	5.0
Ba	0.210	J	100	21
Be		U	1.33	1.22
Cd	0.0635	J	0.48	0.11
Cr		U	29200	0.6
Cu		U	5.0	
Hg		U	0.2	0.025
Ni	0.0325	J	12.1	11.0
Pb		U	5.0	0.75
Sb		U	0.659	1.15
Se		U	1.0	5.7
Tl	0.000023	J	0.282	0.2
V		U	16.9	1.6
Zn	0.325	J	225	4.3

[a] U: the element was not detected in the TCLP solution; J indicates an estimated value that was above the method detection limit, but below the estimated quantitation limit.

[b] UTS limit applies only to Sb, Be, Ni, and Tl, while the US Environmental Protection Agency (EPA) delisting limits apply for the remaining elements.

elements are subjected to the EPA delisting limits. No measurable concentrations were detected for Ag, As, Be, Cr, Cu, Hg, Sb, Se, and V. Of the remaining five elements, concentrations of Ba, Cd, Ni, Tl, and Zn were below the applicable limits (Ba 0.21%, Cd 13%, and Zn 0.14% of the delisting limit; Ni 0.30% and Tl 0.01% of the UTS limit). More details, including quality control data, are in Ref. [10]. The TCLP solution was analyzed also for other elements, but only Al, B, and Ca were present in measurable concentrations – see Table 12. Kot and Pegg [12] report two data sets for the TCLP of HLW98-95 simulant: for Cd, the most TCLP-sensitive component, the reported concentrations are 0.10 and 0.40 g/m^3, values substantially higher than the 0.064 g/m^3 for AZ-101 HLW glass, but still passing the delisting limit of 0.48 g/m^3.

TCLP response of glasses can be estimated with two simple models that predict solution concentrations of congruently released elements. Kim and Vienna's [18] model was developed as a conservative estimate of the B concentration, c_{B}, in the TCLP solution using the formula

$$c_{\mathrm{B}} = g_{\mathrm{B}} \exp \sum_{i=1}^{N-1} \beta_i x_i, \tag{6}$$

where g_{B} is the B mass fraction in glass, β_i is the ith component coefficient listed in Table 13, x_i is the ith component mole fraction in glass, and N is the number of components in the glass.

Table 12
Concentration data and model calculations for elements detected in TCLP solution in g/m^3

	Quenched glass measured	Quenched glass Eq. (6)	Slowly cooled glass Eqs. (1) and (6)	Quenched glass Eq. (7)	Slowly cooled glass Eqs. (1) and (7)
Al	0.225				
B	1.40	2.26	3.28	2.53	2.29
Ba	0.21	0.04	0.06	0.02	0.01
Ca	1.17	0.24	0.35	0.12	0.11
Cd	0.064	0.43	0.62	0.17	0.15
Ni	0.033	0.31	0.08	0.14	0.02
Zn	0.325	1.16	0.15	0.50	0.04

Table 13
TCLP model coefficients

	β_i[a]	k_i[b]
Al_2O_3	−11.830	0.323
B_2O_3	14.155	8.675
CaO	14.266	
CdO		21.667
Fe_2O_3	−9.869	1.014
K_2O	29.025	
Li_2O	10.456	9.406
LN_2O_3[c]	−98.649	
MgO	12.980	
MnO	15.308	6.447
Na_2O	18.440	10.126
Others[d]	9.696	
SiO_2	−1.270	−0.942
SrO	8.975	6.629
ThO_2		−0.597
UO_2		8.776
ZnO		14.311
ZrO_2	−10.114	

[a] Eq. (6) coefficients to obtain c_B in g/m^3 [18].
[b] Eq. (7) coefficients to obtain c_{Cd} in g/m^3 [19].
[c] LN stands for lanthanides.
[d] Others are all remaining glass elements except oxygen.

Kot et al.'s [19] model relates the Cd concentration, c_{Cd} in the TCLP solution as

$$c_{Cd} = g_{CdO}^{b_{CdO}} \exp\left(\frac{\sum_{i=1}^{N} k_i g_i}{\sum_{i=1}^{N} g_i}\right), \quad (7)$$

where $b_{CdO} = 0.9085$ is a constant, and k_i is the ith component coefficient listed in Table 13.

With composition data from Tables 1 and 3, coefficients listed in Table 13, and Eq. (1) for amorphous matrix composition, Eq. (6) yields $c_B = 2.26$ g/m^3 for glass and 3.28 g/m^3 for amorphous matrix, corresponding to $c_{Cd} = 0.43$ g/m^3 for glass and 0.62 g/m^3 for amorphous matrix (with $c_S = 0.071$); Eq. (7) yields, with the same input data, $c_{Cd} = 0.17$ g/m^3 for glass and 0.15 g/m^3 for amorphous matrix. Both models rely on Gan and Peg's [20] observation that all elements listed in Table 12, except Al, are released congruently into the TCLP solution. Table 12 lists the predicted concentrations based on the assumptions of congruency. Both models are conservative with respect to releases of B, Cd, Ni, and Zn. They seemingly underpredict releases of Ba and Ca; the measured value for Ba, the concentration of which in the glass is very low (0.03 mol% BaO), is subjected to a large error; however, the high measured concentration of Ca in the TCLP solution is difficult to understand because its concentration, though low (0.5 mass%), is not extremely low, and its preferential leaching is unlikely.

By Eq. (1), the content of non-spinel components in the amorphous matrix increases with increasing spinel fraction; in particular, the CdO content in the amorphous phase increases from 0.68 mass% to 0.73 mass% when AZ-101 HLW glass precipitates 7.1 mass% spinel. By Eq. (6), concentration of non-spinel congruently dissolving components in TCLP solution would increase 1.4 times in response to spinel precipitation; the spinel-forming components, depending on their partitioning, would significantly decrease (Ni by 78% and Zn by 87%). Spinel dissolution in the TCLP solution is negligible (spinel can be separated from glass by dissolving glass in and acid [21]). By Eq. (7), spinel precipitation would decrease TCLP solution concentrations of all congruently dissolving components (non-spinel components by 9%, Ni by 83%, and Zn by 92%); this impact of spinel precipitation is attributed to the decrease in fractions of amorphous phase constituents (ZnO and MnO) that possess high k_i coefficients (Table 13) in the amorphous matrix.

4. Conclusions

By quantitative XRD analysis, the AZ-101 HLW glass sample subjected to slow cooling contained 7.1 mass% of spinel, predominantly franklinite–trevorite solid solution. Image analysis applied to SEM micrographs resulted in the 3.55 ± 0.50 vol.% of spinel, corresponding to 6.73 ± 0.94 mass%. Most of the crystals

were 0.5–3 μm in size and contained Fe, Ni, Cr, Mn, and Zn. The significantly lower content of spinel (3.4 mass%) in the non-radioactive simulant subjected to the same heat treatment can be attributed to its lower content of spinel-promoting and sparsely soluble components.

The 7-day 90 °C PCT normalized releases of B, Li, and Na from AZ-101 HLW glass subjected to slow cooling were 0.26–0.33 g/m^2. These very low values were 5–11% of the corresponding releases of the EA standard reference glass and are in good agreement with data from the non-radioactive simulant (0.17–0.29 g/m^2).

AZ-101 HLW quenched glass met all TCLP delisting requirements. No measurable concentrations were detected for Ag, As, Be, Cr, Cu, Hg, Sb, Se, and V; concentrations of Ba, Ni, Tl, and Zn were fractions of a percent of applicable limits; the Cd concentration was 13% of the delisting limit (measurements performed on non-radioactive simulant resulted in 20–80% of the delisting limit). Models estimate that spinel precipitation significantly reduces TCLP releases of spinel-forming components, but disagree in the effect of spinel precipitation on congruently dissolving components that do not form spinel.

Acknowledgements

The authors are grateful a number of laboratory staff who enabled this work to be completed and to Wayne Cosby for editorial support. Pacific Northwest National Laboratory is operated for the US Department of Energy by Battelle under Contract DE-AC05-76RL01830.

References

[1] P. Hrma, J.V. Crum, D.J. Bates, P.R. Bredt, L.R. Greenwood, H.D. Smith, these Proceedings.
[2] American Society for Testing and Materials, in: 1998 Annual Book of ASTM Standards, vol. 12.01, West Conshohocken, Pennsylvania, 1998.
[3] US Environmental Protection Agency, Test Methods for Evaluation of Solid Waste Physical/Chemical Methods, SW-846, 3rd. Ed., Washington, DC, 1997.
[4] US Department of Energy, Office of Environmental Management, Waste Acceptance Product Specifications for Vitrified High-Level Waste Form, EM-WAPS Rev. 2, Washington, DC, 1996.
[5] C.M. Jantzen, N.E. Bibler, D.C. Beam, C.L. Crawford, M.A. Pickett, Characterization of the Defense Waste Processing Facility (DWPF) Environmental Assessment (EA) Glass Standard Reference Material, WSRC-TR-92-346, Westinghouse Savannah River Company, Aiken, South Carolina, 1993.
[6] Mineralogy database, 2004. Available from: <http://www.webmineral.com/>.
[7] W.K. Kot, private communication.
[8] J.D. Vienna, D.-S. Kim, P. Hrma, Database and Interim Glass Property Models for Hanford HLW and LAW Glasses, PNNL-14060, Pacific Northwest National Laboratory, Richland, Washington, 2002.
[9] J. Alton, T.J. Plaisted, P. Hrma, J. Non-Cryst. Solids 311 (2002) 24.
[10] P. Hrma, J.V. Crum, D.R. Bates, P.R. Bredt, L.R. Greenwood, H.D. Smith, Vitrification and Product Testing of AZ-101 Pretreated High-Level Waste Envelope D Glass, WTP-RPT-116, Battelle – Pacific Northwest Division, Richland, Washington, 2004.
[11] J.D. Vienna, D.B. Blumenkranz, Preliminary Validation of HLW Simulants and Scale, 24590-HLW-RPT-RT-03-001, Bechtel National, Richland, Washington, 2003.
[12] W.K. Kot, I.L. Pegg, *HLW* Glass Formulation to Support AZ-101 Actual Waste Testing, VSL-02R3770-1, Vitreous State Laboratory, The Catholic University of America, Washington, DC, 2003.
[13] P. Van Iseghem, B. Grambow, in: M.J. Apted, R.E. Westerman (Eds.), Scientific Basis for Nuclear Waste Management XI, Materials Research Society Symposium Proceedings, vol. 112, 1988, p. 631.
[14] P. Hrma, J.D. Vienna, J.D. Yeager, in: S.K. Sundaram et al. (Eds.), Environmental Issues and Waste Management Technologies in the Ceramic and Nuclear Industries VIII, Ceramic Transaction, vol. 143, 2003, p. 245.
[15] B.G. Amidan, G.F. Piepel, D.S. Kim, J.D. Vienna, Statistical Assessment of Bias and Random Uncertainties in WTP HLW CRV Mixing and Sampling, WTP-RPT-126, Battelle – Pacific Northwest Division, Richland, Washington, 2004.
[16] G.F. Piepel, S.K. Cooley, Interim Report: Statistical Assessment of Preliminary Property-Composition Data and Models for IHLW PCT and TCLP, WTP-RPT-045, Battelle – Pacific Northwest Division, Richland, Washington, 2003.
[17] B.J. Riley, P. Hrma, J.A. Rosario, J.D. Vienna, in: G.L. Smith et al. (Eds.), Environmental Issues and Waste Management Technologies in the Ceramic and Nuclear Industries VII, Ceramic Transactions, Westerville, Ohio, vol. 132, 2002, p. 257.
[18] D.-S. Kim, J.D. Vienna, Model for TCLP Releases from Waste Glasses, PNNL-14061, Pacific Northwest National Laboratory, Richland, Washington, 2002.
[19] W.K. Kot, K. Klatt, H. Gan, I.L. Pegg, S.K. Cooley, D.J. Bates, G.F. Piepel, Regulatory Testing of RPP-WTP HLW Glasses for Compliance with Delisting Requirements, VSL-03R3780-1, Vitreous State Laboratory, The Catholic University of America, Washington, DC, 2003.
[20] H. Gan, I.L. Pegg, in: G.L. Smith et al. (Eds.), Environmental Issues and Waste Management Technologies in the Ceramic and Nuclear Industries VII, Ceramic Transaction, vol. 132, 2002, p. 335.
[21] M. Mika, P. Hrma, M.J. Schweiger, Ceramics-Silikaty 44 (2000) 86.